

Unsupervised Few-shot Learning via Deep Laplacian Eigenmaps

Kuilin Chen

University of Toronto

kuilin.chen@mail.utoronto.ca

Chi-Guhn Lee

University of Toronto

cglee@mie.utoronto.ca

Abstract

Learning a new task from a handful of examples remains an open challenge in machine learning. Despite the recent progress in few-shot learning, most methods rely on supervised pretraining or meta-learning on labeled meta-training data and cannot be applied to the case where the pretraining data is unlabeled. In this study, we present an unsupervised few-shot learning method via deep Laplacian eigenmaps. Our method learns representation from unlabeled data by grouping similar samples together and can be intuitively interpreted by random walks on augmented training data. We analytically show how deep Laplacian eigenmaps avoid collapsed representation in unsupervised learning without explicit comparison between positive and negative samples. The proposed method significantly closes the performance gap between supervised and unsupervised few-shot learning. Our method also achieves comparable performance to current state-of-the-art self-supervised learning methods under linear evaluation protocol.

1 Introduction

Few-shot learning (Fei-Fei et al., 2006) aims to learn a new classification or regression model on a novel task that is not seen during training, given only a few examples in the novel task. Existing few-shot learning methods either rely on episodic meta-learning (Finn et al., 2017, Snell et al., 2017) or standard pretraining (Chen et al., 2019, Tian et al., 2020b) in a supervised manner to extract transferable knowledge to a new few-shot task. Unfortunately, these methods require many labeled meta-training samples. Acquiring a lot of labeled data is costly or even impossible in practice. Recently, several unsupervised meta-learning approaches have attempted to address this problem by constructing synthetic tasks on unlabeled meta-training data (Hsu et al., 2019, Khodadadeh et al., 2019, 2021) or meta-training on self-supervised pretrained features (Lee et al., 2021a). However, the performance of unsupervised meta-learning approaches is still far from their supervised counterparts. Empirical studies in supervised pretraining show that representation learning via grouping similar samples together (Chen et al., 2019, Dhillon et al., 2020, Laenen and Bertinetto, 2021, Tian et al., 2020b) outperforms a wide range of episodic meta-learning methods, where the definition of similar samples is given by class labels. The motivation of this study is to develop an unsupervised representation learning method by grouping unlabeled meta-training data without episodic training and close the performance gap between supervised and unsupervised few-shot learning.

Contrastive self-supervised learning has shown remarkable success in learning representation from unlabeled data, which is competitive with supervised learning on multiple visual tasks (Hénaff et al., 2020, Tian et al., 2020a). The common underlying theme behind contrastive learning is to pull together representation of augmented views of the same training sample (positive sam-

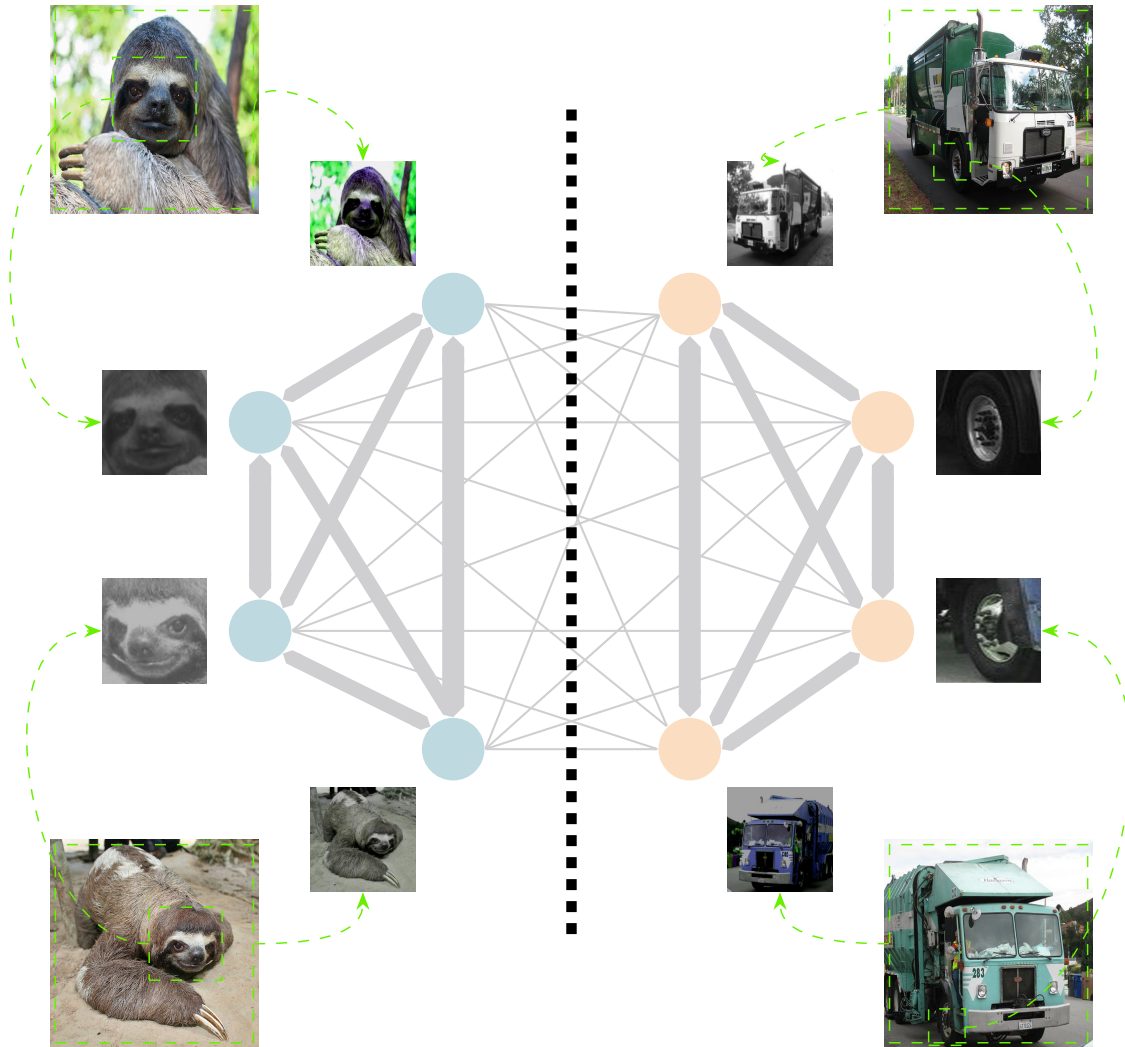


Figure 1: A graph on augmented views of unlabeled training data. The thickness of the edge indicates the transition probability between vertices, which is proportional to their similarity. We group similar vertices together by minimizing the total transition probability between different groups.

ple) and disperse representation of augmented views from different training samples (negative sample) (Wang and Isola, 2020, Wu et al., 2018). Typically, contrastive learning methods require a large size of negative samples to learn high-quality representation from unlabeled data (Chen et al., 2020, He et al., 2020). This inevitably requires a large batch size of samples, demanding significant computing resources. Non-contrastive methods try to overcome the issue by accomplishing self-supervised learning with only positive pairs. However, non-contrastive methods suffer from trivial solutions where the model maps all inputs to the same constant vector, known as the collapsed representation. Various methods have been proposed to avoid collapsed representation on an ad hoc basis, such as asymmetric network architecture (Grill et al., 2020), stop gradient (Chen

and He, 2021), and feature decorrelation (Ermolov et al., 2021, Hua et al., 2021, Zbontar et al., 2021). However, theoretical understanding about how non-contrastive methods avoid collapsed representation is limited, though some preliminary attempts are made to analyze the training dynamics of non-contrastive methods (Tian et al., 2021). Besides, most self-supervised learning methods focus on the linear evaluation task where the training and test data come from the same classes. They do not account for the domain gap between training and test classes, which is the case in few-shot learning and cross-domain few-shot learning.

We develop a novel unsupervised representation learning method in which a weighted graph is used to capture unlabeled samples as nodes and similarity among samples as the weights of edges. Two samples are deemed similar if they are augmentations of a single sample and clustering of samples is accomplished by partitioning the graph. We provide an intuitive understanding of the graph partition problem from the perspective of random walks on the graph, where the transition probability between two vertices is proportional to their similarity. The optimal partition can be found by minimizing the total transition probability between clusters. It is linked to the well-known Laplacian eigenmaps in spectral analysis (Belkin and Niyogi, 2003, Meila and Shi, 2000, Shi and Malik, 2000). We replace the locality-preserving projection in Laplacian eigenmaps with deep neural networks for better scalability and flexibility in learning high-dimensional data such as images.

An additional technique is integrated into deep Laplacian eigenmaps to handle the domain gap between the meta-training and meta-testing sets. Previous studies on word embeddings (e.g. king - man + woman \approx queen) (Mikolov et al., 2013) and disentangled generative models (Karras et al., 2019) show that interpolation between latent embeddings may correspond to the representation of a realistic sample, which may not be seen in the training data. In contrast, interpolation in the input space does not result in realistic samples. In parallel, interpolation between the distributions of the nearest two meta-training classes in the embedding space can approximate the distribution of one meta-testing class after the feature extractor is trained (Yang et al., 2021). To enhance the performance on downstream few-shot learning tasks, we make interpolation of unlabeled meta-training samples on data manifold to mimic unseen meta-test samples and integrate them into unsupervised training of the feature extractor.

Our contributions are summarized as follows:

- A new unsupervised few-shot learning method is developed based on deep Laplacian eigenmaps with an intuitive explanation based on random walks.
- Our loss function is analyzed to show how collapsed representation is avoided without explicit comparison to negative samples, shedding light on existing feature decorrelation based self-supervised learning methods.
- The proposed method significantly closes the performance gap between unsupervised and supervised few-shot learning methods.
- Our method achieves comparable performance to current state-of-the-art (SOTA) self-supervised learning methods under the linear evaluation protocol.

2 Methodology

2.1 Graph from augmented data

First, we construct a graph using augmented views of unlabeled data. Let $\bar{x} \in \mathbb{R}^d$ be a raw sample without augmentation. For image data, augmented views are created by the commonly

used augmentations defined in SimCLR (Chen et al., 2020), including horizontal flip, Gaussian blur, color jittering, and random cropping. \mathcal{X} denotes the set of all augmented data and $N = |\mathcal{X}|$. We represent the augmented data in the form of a weighted graph $\mathcal{G} = (\mathcal{X}, S)$, where each $\mathbf{x} \in \mathcal{X}$ is a vertex of the graph and S denotes the edge weights. The edge between two vertices $\mathbf{x}_i, \mathbf{x}_j \in \mathcal{X}$ is weighted by the non-negative similarity s_{ij} between them. For unrelated \mathbf{x}_i and \mathbf{x}_j , the similarity s_{ij} should be small. On the other hand, the similarity s_{ij} should be large when \mathbf{x}_i and \mathbf{x}_j are augmentations from the same image or augmentations from two images within the same latent classes. An illustrative diagram is shown in Fig. 1.

Let $d_i = \sum_{\mathbf{x}_j \in \mathcal{X}} s_{ij}$ denote the total weights associated with \mathbf{x}_i , which is the degree of a vertex \mathbf{x}_i in a weighted graph. The degree matrix \mathbf{D} is defined as the diagonal matrix with the degrees d_1, \dots, d_N on the diagonal. The volume of \mathcal{X} is $\text{Vol}(\mathcal{X}) = \sum_{\mathbf{x}_i \in \mathcal{X}} d_i$. Similarly, the volume of a subset $C \subset \mathcal{X}$ is defined as $\text{Vol}(C) = \sum_{\mathbf{x}_i \in C} d_i$. Let $\mathbf{P} = \mathbf{D}^{-1}\mathbf{S}$ be the random walk Laplacian of \mathcal{G} , where $p_{ij} = (\mathbf{P})_{ij}$ represents the transition probability from \mathbf{x}_i to \mathbf{x}_j , and each row of \mathbf{P} sums to 1. $\mathbf{L} = \mathbf{D} - \mathbf{S}$ is the unnormalized Laplacian of \mathcal{G} .

2.2 Random walks and graph partition

\mathcal{X} can be grouped into K clusters, where similar vertices should be grouped into the same cluster and dissimilar vertices should be grouped into different clusters. It resembles the supervised pretraining by embedding samples from the same class together. We will show later that K is also the dimension of the embedding. Since we do not know the number of classes in unlabeled training data, we set the embedding dimension $K = 2048$, which works well on a wide range of datasets. Graph partition into clusters can be done by minimizing the total similarity $\sum_{\mathbf{x}_i \in C, \mathbf{x}_j \in C'} s_{ij}$ between two clusters $C, C' \in \mathcal{X}, C \cap C' = \emptyset$. However, minimizing the total inter-cluster similarity is undesirable because it can simply separate one individual vertex from the rest of the graph. Instead, we run random walks on vertices \mathcal{X} .

The random walk Laplacian \mathbf{P} defines a Markov chain on the vertices \mathcal{X} . The stationary distribution π of this chain has an explicit form $\pi_i = d_i / \text{Vol}(\mathcal{X})$ for $\mathbf{x}_i \in \mathcal{X}$ (Meila and Shi, 2000). The transition probability $P(C' | C) = P(X_1 \in C' | X_0 \in C)$ is given by

$$\begin{aligned} & P(X_1 \in C' | X_0 \in C) \\ &= \left(\frac{1}{\text{Vol}(\mathcal{X})} \sum_{\mathbf{x}_i \in C, \mathbf{x}_j \in C'} s_{ij} \right) \left(\frac{\text{Vol}(C)}{\text{Vol}(\mathcal{X})} \right)^{-1} \\ &= \frac{\sum_{\mathbf{x}_i \in C, \mathbf{x}_j \in C'} s_{ij}}{\text{Vol}(C)} \end{aligned} \quad (1)$$

The inter-cluster transition probability is a proper criterion because it has a small value only if $\sum_{\mathbf{x}_i \in C, \mathbf{x}_j \in C'} s_{ij}$ is small (low similarity for vertices in different clusters) and all clusters have sufficiently large volumes. As a result, minimization of the inter-cluster transition probability prevents trivial solutions that simply separate one individual vertex from the rest of the graph.

The inter-cluster transition probability minimizing problem is a constrained optimization problem. For the case of finding K clusters, we define a matrix $\mathbf{Z} \in \mathbb{R}^{N \times K}$, where z_{ik} represents the cluster assignment of the vertex \mathbf{x}_i .

$$z_{ik} = \begin{cases} 1/\sqrt{\text{vol}(C_k)} & \text{if } \mathbf{x}_i \in C_k \\ 0 & \text{otherwise} \end{cases} \quad (2)$$

where $i = 1, \dots, N$ and $k = 1, \dots, K$. Let $\mathbf{z}_{(k)}$ be the k -th column in the matrix \mathbf{Z} . The connection between unnormalized graph Laplacian and inter-cluster transition probability is given by

$$\begin{aligned}
\mathbf{z}_{(k)}^\top \mathbf{L} \mathbf{z}_{(k)} &= \mathbf{z}_{(k)}^\top (\mathbf{D} - \mathbf{S}) \mathbf{z}_{(k)} \\
&= \sum_{i=1}^N d_i z_{ik}^2 - \sum_{i=1}^N \sum_{j=1}^N s_{ij} z_{ik} z_{jk} \\
&= \frac{1}{2} \left(\sum_{i=1}^N d_i z_{ik}^2 - 2 \sum_{i=1}^N \sum_{j=1}^N s_{ij} z_{ik} z_{jk} + \sum_{j=1}^N d_j z_{jk}^2 \right) \\
&= \frac{1}{2} \left(\sum_{i=1}^N \sum_{j=1}^N s_{ij} z_{ik}^2 - 2 \sum_{i=1}^N \sum_{j=1}^N s_{ij} z_{ik} z_{jk} + \sum_{j=1}^N \sum_{i=1}^N s_{ji} z_{jk}^2 \right) \\
&= \frac{1}{2} \sum_{i,j=1}^N s_{ij} (z_{ik} - z_{jk})^2 \\
&= \frac{1}{2} \sum_{i \in C_k, j \in \bar{C}_k} s_{ij} \left(\sqrt{\frac{1}{\text{Vol}(C_k)}} \right)^2 = \frac{1}{2} P(\bar{C}_k | C_k)
\end{aligned} \tag{3}$$

It is easy to verify that $\mathbf{Z}^\top \mathbf{D} \mathbf{Z} = \mathbf{I}$, and $\mathbf{z}_{(k)}^\top \mathbf{D} \mathbf{z}_{(k)} = 1$. We can write the problem of minimizing inter-cluster transition as

$$\begin{aligned}
&\min_{C_1, \dots, C_K} \text{Tr} \left(\mathbf{Z}^\top \mathbf{L} \mathbf{Z} \right) \\
&\text{subject to } \mathbf{Z}^\top \mathbf{D} \mathbf{Z} = \mathbf{I} \\
&\quad z_{ik} = 1/\sqrt{\text{vol}(C_k)} \text{ if } \mathbf{x}_i \in C_k \text{ else } 0
\end{aligned} \tag{4}$$

This problem is NP-hard due to discreteness. Relaxing the discreteness condition, we obtain the relaxed problem

$$\min_{\mathbf{Z} \in \mathbb{R}^{N \times K}} \text{Tr} \left(\mathbf{Z}^\top \mathbf{L} \mathbf{Z} \right) \text{ subject to } \mathbf{Z}^\top \mathbf{D} \mathbf{Z} = \mathbf{I} \tag{5}$$

This is the standard trace minimization problem which is solved when the column space of \mathbf{Z} is the subspace of the K generalized eigenvectors of $\mathbf{L} \mathbf{z} = \lambda \mathbf{D} \mathbf{z}$. The relaxed problem in Eq. (5) leads to the lower bound on the optimal normalized cut of the graph (??) and retains the interpretation of minimizing the transition probability between clusters. In addition, such relaxation has asymptotic behavior when the number of data points tends to infinity (?). As such, rounding \mathbf{Z} leads to cluster indicator because the relaxed problem is a good proxy of the original problem in Eq. (4) (Bach and Jordan, 2006). We actually would not round the continuous \mathbf{Z} as our goal is not clustering. We will learn a linear classifier on \mathbf{Z} in the downstream tasks.

2.3 Deep representation learning

Let $\mathbf{z}_i \in \mathbb{R}^K$ be the i -th row of the matrix \mathbf{Z} . \mathbf{z}_i can serve as desirable representation of \mathbf{x}_i as it exhibits the clustering structure of the graph \mathcal{G} . However, it is not sensible to obtain \mathbf{z}_i by generalized eigenvalue decomposition for two reasons. First, computation of eigenvectors may be prohibitively expensive due to the large size of augmented data \mathcal{X} . Second, it is non-trivial to compute the embeddings for unseen data points in meta-test classes because eigenvalue decomposition is non-parametric (one K -dimensional vector \mathbf{z} is computed for each \mathbf{x} in the training data).

We assume that \mathbf{z} is parametrized by $f_\theta(\mathbf{x})$, where f_θ can be deep neural networks with trainable parameters θ . The relaxed problem in Eq. (5) is converted to

$$\min_{\theta} \text{Tr}(\mathbf{Z}^\top \mathbf{L} \mathbf{Z}) \quad \text{subject to } \mathbf{Z}^\top \mathbf{D} \mathbf{Z} = \mathbf{I} \quad (6)$$

where $\mathbf{Z} = f_\theta(\mathbf{X})$. We design a proper loss function to learn θ that solves the constrained optimization problem in Eq. (6). The trace minimizing can be written as

$$\text{Tr}(\mathbf{Z}^\top \mathbf{L} \mathbf{Z}) = \sum_{\mathbf{x}_i, \mathbf{x}_j \in \mathcal{X}} (s_{ij} \|f(\mathbf{x}_i) - f(\mathbf{x}_j)\|^2) \quad (7)$$

where the summation is taken w.r.t. pairs $(\mathbf{x}_i, \mathbf{x}_j)$ drawn i.i.d. from \mathcal{X} . Note that the similarity s_{ij} for an unrelated pair $(\mathbf{x}_i, \mathbf{x}_j)$ should be negligibly small, compared to the similarity of a related pair $(\mathbf{x}_i, \mathbf{x}_j)$. Therefore, the weighted summation in Eq. (7) can be approximated by summation of the Euclidean distance between the representation of positive pairs within a mini-batch $\mathcal{V}_{\text{batch}}$

$$\mathcal{L}_{\text{trace}} = \mathbb{E}_{\mathbf{z}, \mathbf{z}_+ \in \mathcal{V}_{\text{batch}}} \|\mathbf{z} - \mathbf{z}_+\|^2 \quad (8)$$

where \mathbf{z} and \mathbf{z}_+ are representation of augmented views from the same image. The constraint $\mathbf{Z}^\top \mathbf{D} \mathbf{Z} = \mathbf{I}$ requires the covariance matrix of the representation to be a diagonal matrix. It is equivalent to minimizing the mean squared error on off-diagonal entries of the covariance matrix

$$\mathcal{L}_{\text{const}} = \sum_{k=1}^K \sum_{l \neq k}^K (c_{kl})^2 \quad (9)$$

where $c_{kl} = \sum_{\mathbf{z} \in \mathcal{V}_{\text{batch}}} (\mathbf{z})_k (\mathbf{z})_l / B$ is the covariance between the k -th and l -th dimensions of the feature, B is the size of the mini-batch, and $(\cdot)_k$ denotes the k -th element of a vector.

The total loss is

$$\mathcal{L} = \mathcal{L}_{\text{trace}} + \gamma \mathcal{L}_{\text{const}} \quad (10)$$

where $\mathcal{L}_{\text{trace}}$ comes from trace minimization, $\mathcal{L}_{\text{const}}$ is translated from the constraint on eigenvectors, and γ can be treated as a Lagrange multiplier.

Our method does not require asymmetric twin neural networks, large batch size, large memory bank, or momentum update. It naturally avoids the trivial solution via the orthogonality constraint, which is realized by decorrelating each dimension of the representation. In Section 3, we will provide a more detailed analysis of how collapsed representation is avoided without explicit comparison between positive and negative samples in the loss function.

2.4 Interpolation between unlabeled training samples

The representation of the augmented views can be encoded as $\mathbf{z} = f_\theta(\mathbf{x}) = f_L(g_L(\mathbf{x}))$, where g_L is part of the feature extractor from the input layer to the hidden layer L and f_L is the remaining part of the feature extractor to the output layer. The hidden layer L is randomly selected from a set of eligible layers in the neural network f_θ so that we can interpolate two samples on their intermediate representation. Let \mathbf{x}_i and \mathbf{x}_{i+} be a positive pair. We interpolate intermediate representation $g_L(\mathbf{x}_{i+})$ and $g_L(\mathbf{x}_{j+})$ to get the manifold mixup (Verma et al., 2019) as follows

$$\mathbf{z}_{ij+} = f_L(\lambda g_L(\mathbf{x}_{i+}) + (1 - \lambda)g_L(\mathbf{x}_{j+})) \quad (11)$$

where $\lambda \in [0, 1]$ is a mixing coefficient drawn from a Beta distribution and \mathbf{z}_{ij+} is the mixed representation of \mathbf{x}_{i+} and \mathbf{x}_{j+} after interpolation on the data manifold. \mathbf{z}_{ij+} should match the interpolated representation of \mathbf{z}_i and \mathbf{z}_j in the embedding space with the same mixing coefficient. The trace minimization loss in Eq. (8) can be replaced by

$$\mathcal{L}_{\text{trace}} = \mathbb{E}_{\mathbf{z}, \mathbf{z}_+ \in \mathcal{V}_{\text{batch}}} \|(\lambda \mathbf{z}_i + (1 - \lambda)\mathbf{z}_j) - \mathbf{z}_{ij+}\|^2 \quad (12)$$

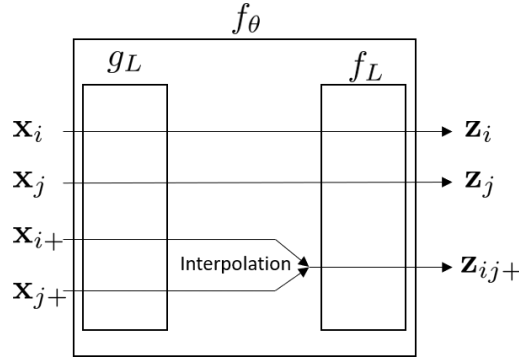


Figure 2: Interpolation of unlabeled training data on data manifold.

An illustrative diagram can be found in Fig. 2. The pseudo-code is presented in Algorithm 1.

Algorithm 1 Pseudo-code of deep Laplacian eigenmaps in a PyTorch-like style.

```

# B      : batch size
# K      : representation dim
# d_x    : input dim
# x      : Tensor, shape=[B, d_x]
#        : augmented views
# x_p    : Tensor, shape=[B, d_x]
#        : positive pairs of x
# z      : Tensor, shape=[B, K]
#        : representation of augmented views
# z_p    : Tensor, shape=[B, K]
#        : positive pairs of z
# gamma  : hyperparameter balancing the two losses
# lambda : interpolation coefficient
# f_theta : feature extractor
# L      : an randomly selected layer
# g_L    : first L layers of f_theta
# f_L    : remaining layers of f_theta
# off_diag: off-diagonal elements of a matrix

def similarity(z, z_p):
    return (z - z_p).pow(2).mean()

def decorrelation(z):
    c = z.T @ z / B
    decorr_loss = off_diag(c).pow(2).sum()

z = f_theta(x)
permuted_index = randperm(B)
manifold_mix = lambda * g_L(x_p)
                + (1 - lambda) * g_L(x_p[permuted_index])
z_p_mix = f_L(manifold_mix)
z_mix = lambda * z + (1 - lambda) * z[permuted_index]
loss = similarity(z_mix, z_p_mix) + gamma * decorrelation(z)

```

3 Unravel feature decorrelation

We analyze the feature decorrelation loss in Eq. (9) and show that feature decorrelation is indeed mathematically equivalent to contrasting between positive and negative samples. At first glance, the off-diagonal entries have nothing to do with the inner product between the representation of positive and negative samples. Previous works (Hua et al., 2021, Zbontar et al., 2021) provide qualitative and empirical analysis to show that feature decorrelation avoids collapsed representation. To the best of our knowledge, we are the first to shed light on the equivalence and analyze the gradient of the feature decorrelation loss.

When each dimension of \mathbf{Z} is standardized to zero mean and unit variance (due to the final batch normalization layer), the diagonal entries of the covariance matrix \mathbf{C} become constant $c_{ii} = 1$. Minimizing the square of off-diagonal entries in Eq. (9) is equivalent to minimizing the Frobenius norm of the covariance matrix,

$$\begin{aligned}
\|\mathbf{C}\|_F^2 &= \frac{1}{N^2} \|\mathbf{Z}^\top \mathbf{Z}\|_F^2 = \frac{1}{N^2} \text{tr} \left(\mathbf{Z}^\top \mathbf{Z} \left(\mathbf{Z}^\top \mathbf{Z} \right)^\top \right) \\
&= \frac{1}{N^2} \text{tr} \left(\mathbf{Z} \mathbf{Z}^\top \mathbf{Z} \mathbf{Z}^\top \right) = \frac{1}{N^2} \text{tr} \left(\left(\mathbf{Z} \mathbf{Z}^\top \right)^\top \mathbf{Z} \mathbf{Z}^\top \right) \\
&= \frac{1}{N^2} \sum_{i=1}^N \sum_{j=1}^N \left(\left(\mathbf{Z} \mathbf{Z}^\top \right) \circ \left(\mathbf{Z} \mathbf{Z}^\top \right) \right)_{ij} \\
&= \frac{1}{N^2} \sum_{i=1}^N \sum_{j=1}^N \left(f_\theta(\mathbf{x}_i)^\top f_\theta(\mathbf{x}_j) \right)^2
\end{aligned} \tag{13}$$

where \circ denotes the Hadamard product. The second line of Eq. (13) is based on the cyclic property of the trace operation and the fact that $\mathbf{Z} \mathbf{Z}^\top$ is symmetric. After rewriting the trace operation via the Hadamard product, we have the final expression, showing that the squared Frobenius norm of the covariance matrix can be expressed as a summation over the squared inner product between pairs of representation. Note that $\mathbf{z}_i = f_\theta(\mathbf{x}_i)$ is usually projected to a sphere ball with a radius of 1 in self-supervised learning. The inner product between the representation of the same augmented view is constant $\mathbf{z}_i^\top \mathbf{z}_i = 1$. Minimizing the square of off-diagonal entries in Eq. (9) is equivalent to minimizing the total squared cosine similarity between random pairs.

After demystifying the feature decorrelation loss, we can analyze the gradient of our loss function to show how it pulls similar samples together and pushes dissimilar samples apart. Let \mathbf{z}_i be the anchor sample, \mathbf{z}_{i+} be a positive sample, and \mathbf{z}_j be an unspecified sample in the current batch $\mathcal{V}_{\text{batch}}$. The gradient with respect to the anchor sample is given by

$$\frac{\partial \mathcal{L}}{\partial \mathbf{z}_i} = \frac{2}{B} \left((1 - \gamma) \mathbf{z}_i - \mathbf{z}_{i+} + \gamma \sum_{\mathbf{z}_j \in \mathcal{V}_{\text{batch}}} \frac{\mathbf{z}_i^\top \mathbf{z}_j}{B} \mathbf{z}_j \right) \tag{14}$$

where B is the size of the mini-batch. Since γ is a small positive number, the gradient can be further simplified as $\frac{\partial \mathcal{L}}{\partial \mathbf{z}_i} = \frac{2}{B} \left((\mathbf{z}_i - \mathbf{z}_{i+}) + \gamma \sum_{\mathbf{z}_j \in \mathcal{V}_{\text{batch}}} \omega_j \mathbf{z}_j \right)$, where ω_j is a weighting factor for negative samples which is proportional to the similarity between the positive and negative samples. The first term of the gradient pulls positive pairs together while the second term disperses the negative samples.

4 Related Work

Few-shot learning is cast to optimization-based (Antoniou et al., 2018, Bertinetto et al., 2019, Finn et al., 2017, Flennerhag et al., 2020, Lee and Choi, 2018, Nichol et al., 2018, Park and Oliva, 2019, Ravi and Larochelle, 2017, Rusu et al., 2019) or metric-based (Koch et al., 2015, Oreshkin et al., 2018, Qi et al., 2018, Snell et al., 2017, Sung et al., 2018, Vinyals et al., 2016, Yoon et al., 2019, 2020) meta-learning problems through supervised episodic training because it mimics the circumstances encountered in few-shot learning. The model is trained by a series of learning episodes, each of which consists of a limited number of support (training) samples and query (validation) samples.

Nevertheless, simple baselines can outperform SOTA episodic meta-learning methods by using embeddings pre-trained with standard supervised learning (Chen et al., 2019, Dhillon et al., 2020, Laenen and Bertinetto, 2021, Mangla et al., 2020, Tian et al., 2020b). Although episodic meta-learning methods can be applied to unlabeled meta-training data by constructing synthetic tasks (Hsu et al., 2019, Khodadadeh et al., 2019, 2021) or modeling the multi-modality within each randomly sampled episode (Lee et al., 2021a), the performance is much worse than the supervised counterparts. Different from established few-shot learning methods, our method learns useful representation for downstream few-shot learning tasks using unlabeled meta-training data without episodic training.

Contrastive learning with variants of InfoNCE loss (Gutmann and Hyvärinen, 2010, Oord et al., 2018) has been widely used in self-supervised/unsupervised representation learning (Chen et al., 2020, He et al., 2020, Hénaff et al., 2020, Wu et al., 2018). It is derived from the maximization of the mutual information (MI) between related views (Poole et al., 2019). However, this interpretation could be inconsistent with some empirical observations in self-supervised learning, such as tighter lower bounds of MI leading to worse performance (McAllester and Stratos, 2020, Tschannen et al., 2020, Wang and Isola, 2020). The InfoNCE loss can be expressed as $\mathcal{L}_{\text{InfoNCE}} = -\sum_i \log \frac{\exp(\mathbf{z}_i^\top \mathbf{z}_{i+}/\tau)}{\sum_{\mathbf{z}_j \in \mathcal{V}} \exp(\mathbf{z}_i^\top \mathbf{z}_j/\tau)}$, where \mathcal{V} can be a mini-batch or a memory bank. The core idea of contrastive learning is pulling positive pairs together while pushing negative samples apart (Wang and Isola, 2020). It can be easily verified from the gradient $\frac{\partial \mathcal{L}_{\text{InfoNCE}}}{\partial \mathbf{z}_i} = (-\mathbf{z}_{i+} + \sum_{\mathbf{z}_j \in \mathcal{V}} \omega_j \mathbf{z}_j)/\tau$, where $\omega_j = \frac{\exp(\mathbf{z}_i^\top \mathbf{z}_j/\tau)}{\sum_{\mathbf{z}_j \in \mathcal{V}} \exp(\mathbf{z}_i^\top \mathbf{z}_j/\tau)}$ is a weighting factor that is proportional to the similarity between the anchor sample \mathbf{z}_i and the negative sample \mathbf{z}_j . Our method shares a similar form of the gradient with a different weighting scheme on negative samples, though our loss function is derived from a different perspective. Recent studies show that weighting schemes on negative samples affect the learning efficiency with respect to the negative sample size (Wang and Liu, 2021, Yeh et al., 2021). Compared with contrastive learning with InfoNCE loss, our method does not require a large size of negative samples to work well.

Clustering methods have been employed in self-supervised learning (Asano et al., 2019, Caron et al., 2018, 2020) by simultaneously clustering the unlabeled data while enforcing consistent cluster assignments for different augmented views of the same image. These methods do not compare positive and negative samples directly as in contrastive learning, but careful implementation details and large batches are necessary because clustering methods are prone to collapse. The derivation of our method resembles spectral clustering but our method does not perform clustering. Unsupervised representation learning via deep Laplacian eigenmaps can be intuitively interpreted by random walks on augmented views of unlabeled data and use deep neural networks to handle high-dimensional image data. Random walks on image pixels have been developed to solve a supervised image segmentation problem by minimizing the Kullback-Leibler divergence between the learned transition probability and the target transition probability (Meila and Shi, 2000). If f_θ is a linear function, the linear projection is locality preserving (He and Niyogi, 2004).

Feature decorrelation methods avoid collapsed representation in self-supervised learning without using a large number of negative samples. Feature decorrelation can be achieved by differentiable Cholesky decomposition on each batch of embeddings (Ermolov et al., 2021), forcing the cross-correlation matrix of representations close to the identity matrix (Zbontar et al., 2021), or utilization of decorrelated batch normalization with a shuffling operation (Hua et al., 2021). Feature decorrelation methods show comparable performance to contrastive learning methods, but the fundamental principle behind it is unclear. Although Barlow Twins (Zbontar et al., 2021) are derived from the information bottleneck principle, it is only valid for Gaussian distributed data. The

loss function in our method is similar to those in decorrelation methods. However, our method is derived from the well-known spectral analysis of the Laplacian matrix and requires minimal assumptions about the training data. Existing feature decorrelation methods in self-supervised learning can be unified in our framework - a trace minimization problem with orthogonality constraints, with minor differences in handling orthogonality constraints in practice. We also show the exact reason why feature decorrelation avoids collapsed representation.

Mixup (Zhang et al., 2018) and its variants (Verma et al., 2019, Yun et al., 2019) provide effective data augmentation strategies to improve performance in supervised learning. Mixing up the image pixels has been explored in self-supervised learning (Lee et al., 2021b, Shen et al., 2022). MoChi (Kalantidis et al., 2020) mixes the final representation of negative samples to create hard negative samples. Our method mixes up the intermediate representation to achieve better empirical performance.

5 Experiments

We evaluate the performance of our model trained on unlabeled meta-training data on few-shot learning tasks, including in-domain and more challenging cross-domain settings. In addition, our method is also compared with SOTA self-supervised learning method under linear evaluation protocol to show that the proposed method can be applied to a wide range of downstream tasks beyond few-shot learning.

5.1 Few-shot classification

We conduct few-shot classification experiments on three widely used few-shot image recognition benchmarks.

miniImageNet is a 100-class subset of the original ImageNet dataset (Deng et al., 2009) for few-shot learning (Vinyals et al., 2016). miniImageNet is split into 64 training classes, 16 validation classes, and 20 testing classes, following the widely used data splitting protocol (Ravi and Larochelle, 2017).

FC100 is a derivative of CIFAR-100 with minimized overlapped information between train classes and test classes by grouping the 100 classes into 20 superclasses (Oreshkin et al., 2018). They are further split into 60 training classes (12 superclasses), 20 validation classes (4 superclasses), and 20 test classes (4 superclasses).

miniImageNet to CUB is a cross-domain few-shot classification task, where the models are trained on miniImageNet and tested on CUB (Welinder et al., 2010). Cross-domain few-shot classification is more challenging due to the big domain gap between two datasets. We can better evaluate the generalization capability in different algorithms. We follow the experiment setup in (Yue et al., 2020).

The feature extractor f_θ contains two components: a backbone network and a projection network. The backbone network can be a variant of ResNet architecture (He et al., 2016). The projection network is a 3-layer MLP with batch normalization and ReLU activation. The dimension of each layer in the projection MLP is 2048. We use the same augmentations defined in SimCLR (Chen et al., 2020), including horizontal flip, Gaussian blur, color jittering, and random cropping.

We use ResNet12 (Lee et al., 2019, Ravichandran et al., 2019) and WRN-28-10 (Yue et al., 2020) as the backbone networks for few-shot learning and cross-domain few-shot learning, respectively. Those two backbone networks are selected because they are widely used in SOTA few-shot learning methods. The feature extractor is trained on unlabeled meta-training data by the SGD optimizer

(momentum of 0.9 and weight decay of $5e-4$) with a mini-batch size of 128. The learning rate starts at 0.05 and decreases to 0 with a cosine schedule. The projection network in the feature extractor is discarded after training on unlabeled data.

During meta-testing, we train a regularized logistic regression model using 1×5 or 5×5 support samples on frozen representations after the global average pooling layer in the backbone network. Each few-shot task contains 5 classes and 75 query samples. The classification accuracy is evaluated on the query samples.

Table 1: Few-shot classification results on miniImageNet and FC100.

Method	Backbone	miniImageNet 5-way		FC100 5-way	
		1-shot	5-shot	1-shot	5-shot
Supervised					
Proto Net (Snell et al., 2017)	ResNet-12	60.37 ± 0.83	78.02 ± 0.57	41.5 ± 0.7	57.0 ± 0.7
MAML (Finn et al., 2017)	ResNet-12	56.58 ± 1.84	70.85 ± 0.91	36.9 ± 0.6	51.2 ± 0.7
TADAM (Oreshkin et al., 2018)	ResNet-12	58.50 ± 0.30	76.70 ± 0.30	40.1 ± 0.4	56.1 ± 0.4
Baseline++ (Chen et al., 2019)	ResNet-12	60.83 ± 0.81	77.81 ± 0.76	41.3 ± 0.7	58.7 ± 0.7
MetaOptNet (Lee et al., 2019)	ResNet-12	62.64 ± 0.61	78.63 ± 0.46	41.1 ± 0.6	55.5 ± 0.6
Unsupervised					
CACTUs-MAML (Hsu et al., 2019)	ResNet-12	49.41 ± 0.92	63.72 ± 0.83	31.3 ± 0.8	45.7 ± 0.8
UMTRA (Khodadadeh et al., 2019)	ResNet-12	49.62 ± 0.91	62.43 ± 0.84	31.5 ± 0.8	45.3 ± 0.8
Meta-GMVAE (Lee et al., 2021a)	ResNet-12	55.93 ± 0.85	74.28 ± 0.72	36.3 ± 0.7	49.7 ± 0.7
SimCLR (Chen et al., 2020)	ResNet-12	55.76 ± 0.88	75.59 ± 0.69	36.2 ± 0.7	49.9 ± 0.7
MoCo v2 (He et al., 2020)	ResNet-12	57.73 ± 0.84	77.51 ± 0.63	37.7 ± 0.7	53.2 ± 0.7
BYOL (Grill et al., 2020)	ResNet-12	56.17 ± 0.89	76.17 ± 0.66	37.2 ± 0.7	52.8 ± 0.6
Barlow Twins (Zbontar et al., 2021)	ResNet-12	57.79 ± 0.89	77.42 ± 0.66	37.9 ± 0.7	54.1 ± 0.6
Ours	ResNet-12	59.47 ± 0.87	78.79 ± 0.58	39.7 ± 0.7	57.9 ± 0.7

The results of the proposed method and previous few-shot learning methods using similar backbones are reported in Table 1. The proposed method outperforms existing unsupervised few-shot learning methods such as CACTUS (Hsu et al., 2019) and UMTRA (Khodadadeh et al., 2019) by a large margin. It demonstrates that high-quality representation for downstream few-shot tasks can be learned from unlabeled meta-training data without episodic training. Our method is in the category of self-supervised representation learning like SimCLR (Chen et al., 2020), MoCo v2 (He et al., 2020), BYOL (Grill et al., 2020), and Barlow Twins (Zbontar et al., 2021) as it does not perform episodic learning. SimCLR achieves weaker performance than other self-supervised learning methods because it typically requires very large batch sizes to perform well. Although Meta-GMVAE (Lee et al., 2021a) performs unsupervised meta-learning on top of the pretrained features from SimCLR, the performance gain versus vanilla representation from SimCLR is at most marginal when deep backbones are used in our reproduction. This observation aligns with the empirical results in supervised few-shot learning where the advantage of episodic meta-learning diminishes as the backbone becomes deep (Chen et al., 2019, Tian et al., 2020b). Our method is also compared with some strong baselines in supervised few-shot learning. The performance gap between supervised and unsupervised few-shot learning is significantly reduced by our method, compared with previ-

Table 2: Cross-domain few-shot classification results on miniImageNet to CUB.

Method	Backbone	miniImageNet to CUB 5-way	
		1-shot	5-shot
Supervised			
MAML (Finn et al., 2017)	WRN-28-10	39.06 ± 0.47	55.04 ± 0.42
LEO (Rusu et al., 2019)	WRN-28-10	41.45 ± 0.54	56.66 ± 0.48
MTL (Sun et al., 2019)	WRN-28-10	43.15 ± 0.44	56.89 ± 0.41
Matching Net (Vinyals et al., 2016)	WRN-28-10	42.04 ± 0.57	53.08 ± 0.45
SIB (Hu et al., 2020)	WRN-28-10	43.27 ± 0.44	59.94 ± 0.42
Baseline (Chen et al., 2019)	WRN-28-10	42.89 ± 0.41	62.12 ± 0.40
Unsupervised			
CACTUs-MAML (Hsu et al., 2019)	WRN-28-10	33.48 ± 0.49	49.97 ± 0.41
UMTRA (Khodadadeh et al., 2019)	WRN-28-10	33.59 ± 0.48	50.21 ± 0.45
Meta-GMVAE (Lee et al., 2021a)	WRN-28-10	38.09 ± 0.47	55.65 ± 0.42
SimCLR (Chen et al., 2020)	WRN-28-10	38.25 ± 0.49	55.89 ± 0.46
MoCo v2 (He et al., 2020)	WRN-28-10	39.29 ± 0.47	56.49 ± 0.44
BYOL (Grill et al., 2020)	WRN-28-10	40.63 ± 0.46	56.92 ± 0.43
Barlow Twins (Zbontar et al., 2021)	WRN-28-10	40.46 ± 0.47	57.16 ± 0.42
Ours	WRN-28-10	41.08 ± 0.48	58.86 ± 0.45

ous results in unsupervised few-shot learning (Hsu et al., 2019, Khodadadeh et al., 2019, Lee et al., 2021a).

Our method is also applied to the cross-domain few-shot classification task as summarized in Table 2. The proposed method outperforms other unsupervised methods in this challenging task, indicating that the learned representation has strong generalization capability. We use the same hyperparameters (training epochs, learning rate, etc.) from in-domain few-shot learning to train the model. The strong results indicate that our method is robust to hyperparameter choice. Although meta-learning methods with adaptive embeddings are expected to perform better than a fixed embedding when the domain gap between base classes and novel classes is large, empirical results show that a fixed embedding from supervised or unsupervised pretraining achieves better performance in both cases. (Tian et al., 2020b) also reports similar results that a fixed embedding from supervised pretraining shows superior performance on a large-scale cross-domain few-shot classification dataset. We still believe that adaptive embeddings should be helpful when the domain gap between base and novel classes is large. Nevertheless, how to properly train a model on unlabeled meta-training training to obtain useful adaptive embeddings in novel tasks is an open question.

Ablation studies are conducted to analyze how individual components affect the performance of few-shot learning. We study four variants of our methods: (a) the model is trained by only minimizing the similarity between positive pairs $\mathcal{L}_{\text{trace}}$; (b) the projector network is a 2-layer MLP; (c) manifold mixup is not used in the model; (d) manifold mixup is replaced by input mixup. Table 3 shows the results of our ablation studies on FC100. When the model is trained without feature decorrelation, the accuracy on few-shot learning is close to random guess. It indicates that feature decorrelation is the key to avoiding trivial representation in learning from unlabeled data. After

replacing the projector network with a 2-layer MLP, we can see obvious performance loss in the proposed method. Sufficient depth in the projector network is required to achieve optimal performance. The performance deteriorates without manifold mixup, indicating that manifold mixup helps the model to learn task-relevant information for downstream meta-test tasks. Compared with manifold mixup, input mixup is less effective in improving the few-shot learning performance.

Table 3: Ablation studies on FC100.

	FC100 5-way	
	1-shot	5-shot
Only $\mathcal{L}_{\text{trace}}$	Collapsed	Collapsed
2-layer MLP	36.1 ± 0.7	50.2 ± 0.7
Remove manifold mixup	38.2 ± 0.7	54.4 ± 0.7
Use input mixup	38.7 ± 0.7	55.6 ± 0.7
Ours	39.7 ± 0.7	57.9 ± 0.7

5.2 Linear evaluation

To examine the quality of the learned representation, we follow the linear evaluation protocol in self-supervised learning. After the feature extractor is pretrained by unlabeled training data, a linear classifier is trained on top of the frozen backbone network using the labeled training data. The linear evaluation performance is widely used as the proxy for representation quality because it is highly correlated to the performance in downstream tasks, such as transfer learning, objection detection, and image segmentation (Chen and He, 2021, He et al., 2020). Different from few-shot learning, unlabeled training data, labeled training data, and test data are from the same classes under the linear evaluation protocol. We conduct experiments on CIFAR-10/100 and STL-10.

CIFAR-10/100 are two datasets of tiny natural images with a size 32×32 (Krizhevsky, 2009). CIFAR-10 and CIFAR-100 have 10 and 100 classes, respectively. Both datasets contain 50,000 training images and 10,000 test images.

STL-10 is a 10-class image recognition dataset for unsupervised learning (Coates et al., 2011). Each class contains 500 labeled training images and 800 test images. In addition, it also contains 100,000 unlabeled training images. Both labeled and unlabeled training images are used for feature extractor pretraining without using labels. The linear classifier is learned using the labeled training images.

ResNet18 is adopted as the backbone network in the feature extractor. We train the feature extractor using SGD with momentum of 0.9 and weight decay of $5e-4$. The learning rate starts at 0.05 and decreases to 0 with a cosine schedule. The feature extractor is trained for 800 epochs with a batch size of 256.

After the feature extractor is pretrained by unlabeled data, a linear classifier is trained using SGD with a batch size of 256 and no weight decay for 100 epochs. The learning rate starts at 30.0 and is decayed by 0.1 at the 60th and 80th epochs. The test accuracy is reported in Table 4.

Our approach achieves comparable performance to SOTA self-supervised learning methods in the linear evaluation under the same training recipe. Considering the good performance in linear evaluation, our method can be used in a wide range of downstream tasks beyond few-shot learning.

Table 4: Accuracy under linear evaluation protocol

	CIFAR-10	CIFAR-100	STL-10
SimCLR	90.57	63.84	87.52
MoCo v2	90.67	64.13	87.71
BYOL	91.74	65.92	88.46
Barlow Twins	91.58	65.83	88.65
Ours	92.24	66.16	88.97

6 Conclusions

In this article, we propose a new unsupervised few-shot learning method via deep Laplacian eigenmaps. Our method learns representation from unlabeled data by grouping similar samples together and can be intuitively interpreted by random walks on augmented training data. We provide a detailed analysis of our loss function derived from constrained trace minimization to show how it avoids collapsed representation analytically and the connection to existing self-supervised learning methods. The few-shot learning performance benefits from the interpolation of unlabeled training samples on the data manifold. Compared with existing unsupervised few-shot learning methods, the performance gap to supervised few-shot learning methods is significantly narrowed. Additional results on linear evaluation suggest that our method can be applied to a wide range of downstream tasks beyond few-shot classification.

References

- Antreas Antoniou, Harrison Edwards, and Amos Storkey. How to train your maml. In *International Conference on Learning Representations*, 2018.
- YM Asano, C Rupprecht, and A Vedaldi. Self-labelling via simultaneous clustering and representation learning. In *International Conference on Learning Representations*, 2019.
- Francis R Bach and Michael I Jordan. Learning spectral clustering, with application to speech separation. *The Journal of Machine Learning Research*, 7:1963–2001, 2006.
- Mikhail Belkin and Partha Niyogi. Laplacian eigenmaps for dimensionality reduction and data representation. *Neural computation*, 15(6):1373–1396, 2003.
- Luca Bertinetto, Joao F Henriques, Philip Torr, and Andrea Vedaldi. Meta-learning with differentiable closed-form solvers. In *International Conference on Learning Representations*, 2019.
- Mathilde Caron, Piotr Bojanowski, Armand Joulin, and Matthijs Douze. Deep clustering for unsupervised learning of visual features. In *Proceedings of the European Conference on Computer Vision (ECCV)*, pages 132–149, 2018.
- Mathilde Caron, Ishan Misra, Julien Mairal, Priya Goyal, Piotr Bojanowski, and Armand Joulin. Unsupervised learning of visual features by contrasting cluster assignments. In *Advances in Neural Information Processing Systems 33: Annual Conference on Neural Information Processing Systems 2020, NeurIPS 2020, December 6-12, 2020, virtual*, 2020.
- Ting Chen, Simon Kornblith, Mohammad Norouzi, and Geoffrey Hinton. A simple framework for contrastive learning of visual representations. In *International conference on machine learning*, pages 1597–1607. PMLR, 2020.

- Wei-Yu Chen, Yen-Cheng Liu, Zsolt Kira, Yu-Chiang Frank Wang, and Jia-Bin Huang. A closer look at few-shot classification. In *International Conference on Learning Representations*, 2019.
- Xinlei Chen and Kaiming He. Exploring simple siamese representation learning. In *Proceedings of the IEEE/CVF Conference on Computer Vision and Pattern Recognition*, 2021.
- Adam Coates, Andrew Ng, and Honglak Lee. An Analysis of Single Layer Networks in Unsupervised Feature Learning. In *AISTATS*, 2011.
- Jia Deng, Wei Dong, Richard Socher, Li-Jia Li, Kai Li, and Li Fei-Fei. Imagenet: A large-scale hierarchical image database. In *2009 IEEE conference on computer vision and pattern recognition*, pages 248–255. Ieee, 2009.
- Guneet Singh Dhillon, Pratik Chaudhari, Avinash Ravichandran, and Stefano Soatto. A baseline for few-shot image classification. In *International Conference on Learning Representations*, 2020.
- Aleksandr Ermolov, Aliaksandr Siarohin, Enver Sangineto, and Nicu Sebe. Whitening for self-supervised representation learning. In *International Conference on Machine Learning*, pages 3015–3024. PMLR, 2021.
- Li Fei-Fei, Rob Fergus, and Pietro Perona. One-shot learning of object categories. *IEEE transactions on pattern analysis and machine intelligence*, 28(4):594–611, 2006.
- Chelsea Finn, Pieter Abbeel, and Sergey Levine. Model-agnostic meta-learning for fast adaptation of deep networks. In *Proceedings of the 34th International Conference on Machine Learning-Volume 70*, pages 1126–1135. JMLR. org, 2017.
- Sebastian Flennerhag, Andrei A Rusu, Razvan Pascanu, Francesco Visin, Hujun Yin, and Raia Hadsell. Meta-learning with warped gradient descent. In *International Conference on Learning Representations*, 2020.
- Jean-Bastien Grill, Florian Strub, Florent Althé, Corentin Tallec, Pierre H Richemond, Elena Buchatskaya, Carl Doersch, Bernardo Avila Pires, Zhaohan Daniel Guo, Mohammad Gheshlaghi Azar, et al. Bootstrap your own latent: A new approach to self-supervised learning. In *Proceedings of the 33rd International Conference on Neural Information Processing Systems*, 2020.
- Michael Gutmann and Aapo Hyvärinen. Noise-contrastive estimation: A new estimation principle for unnormalized statistical models. In *Proceedings of the thirteenth international conference on artificial intelligence and statistics*, pages 297–304, 2010.
- Kaiming He, Xiangyu Zhang, Shaoqing Ren, and Jian Sun. Deep residual learning for image recognition. In *Proceedings of the IEEE conference on computer vision and pattern recognition*, pages 770–778, 2016.
- Kaiming He, Haoqi Fan, Yuxin Wu, Saining Xie, and Ross Girshick. Momentum contrast for unsupervised visual representation learning. In *Proceedings of the IEEE/CVF Conference on Computer Vision and Pattern Recognition*, pages 9729–9738, 2020.
- Xiaofei He and Partha Niyogi. Locality preserving projections. In *Advances in neural information processing systems*, volume 16, pages 153–160, 2004.
- Olivier J Hénaff, Aravind Srinivas, Jeffrey De Fauw, Ali Razavi, Carl Doersch, SM Eslami, and Aaron van den Oord. Data-efficient image recognition with contrastive predictive coding. In *International Conference on Machine Learning*, pages 4182–4192. PMLR, 2020.

- Kyle Hsu, Sergey Levine, and Chelsea Finn. Unsupervised learning via meta-learning. In *International Conference on Learning Representations*, 2019.
- Shell Xu Hu, Pablo Garcia Moreno, Yang Xiao, Xi Shen, Guillaume Obozinski, Neil Lawrence, and Andreas Damianou. Empirical bayes transductive meta-learning with synthetic gradients. In *International Conference on Learning Representations*, 2020.
- Tianyu Hua, Wenxiao Wang, Zihui Xue, Sucheng Ren, Yue Wang, and Hang Zhao. On feature decorrelation in self-supervised learning. In *Proceedings of the IEEE/CVF International Conference on Computer Vision*, pages 9598–9608, 2021.
- Yannis Kalantidis, Mert Bülent Sariyildiz, Noé Pion, Philippe Weinzaepfel, and Diane Larlus. Hard negative mixing for contrastive learning. In *Advances in Neural Information Processing Systems 33: Annual Conference on Neural Information Processing Systems 2020, NeurIPS 2020, December 6-12, 2020, virtual*, 2020.
- Tero Karras, Samuli Laine, and Timo Aila. A style-based generator architecture for generative adversarial networks. In *Proceedings of the IEEE/CVF Conference on Computer Vision and Pattern Recognition*, pages 4401–4410, 2019.
- Siavash Khodadadeh, Ladislau Boloni, and Mubarak Shah. Unsupervised meta-learning for few-shot image classification. In *Advances in neural information processing systems*, 2019.
- Siavash Khodadadeh, Sharare Zehtabian, Saeed Vahidian, Weijia Wang, Bill Lin, and Ladislau Boloni. Unsupervised meta-learning through latent-space interpolation in generative models. In *International Conference on Learning Representations*, 2021.
- Gregory Koch, Richard Zemel, and Ruslan Salakhutdinov. Siamese neural networks for one-shot image recognition. In *ICML deep learning workshop*, volume 2. Lille, 2015.
- A Krizhevsky. *Learning Multiple Layers of Features from Tiny Images*. PhD thesis, University of Toronto, 2009.
- Steinar Laenen and Luca Bertinetto. On episodes, prototypical networks, and few-shot learning. In *Advances in Neural Information Processing Systems*, 2021.
- Dong Bok Lee, Dongchan Min, Seanie Lee, and Sung Ju Hwang. Meta-gmvae: Mixture of gaussian vae for unsupervised meta-learning. In *International Conference on Learning Representations*, 2021a.
- Kibok Lee, Yian Zhu, Kihyuk Sohn, Chun-Liang Li, Jinwoo Shin, and Honglak Lee. $\$i\$$ -mix: A domain-agnostic strategy for contrastive representation learning. In *International Conference on Learning Representations*, 2021b.
- Kwonjoon Lee, Subhransu Maji, Avinash Ravichandran, and Stefano Soatto. Meta-learning with differentiable convex optimization. In *Proceedings of the IEEE Conference on Computer Vision and Pattern Recognition*, pages 10657–10665, 2019.
- Yoonho Lee and Seungjin Choi. Gradient-based meta-learning with learned layerwise metric and subspace. In *International Conference on Machine Learning*, pages 2927–2936, 2018.
- Puneet Mangla, Mayank Singh, Abhishek Sinha, Nupur Kumari, Vineeth N Balasubramanian, and Balaji Krishnamurthy. Charting the right manifold: Manifold mixup for few-shot learning. In *2020 IEEE Winter Conference on Applications of Computer Vision (WACV)*, pages 2207–2216. IEEE, 2020.

- David McAllester and Karl Stratos. Formal limitations on the measurement of mutual information. In *International Conference on Artificial Intelligence and Statistics*, pages 875–884. PMLR, 2020.
- Marina Meila and Jianbo Shi. Learning segmentation by random walks. In *Advances in neural information processing systems*, volume 13, pages 873–879, 2000.
- Tomás Mikolov, Kai Chen, Greg Corrado, and Jeffrey Dean. Efficient estimation of word representations in vector space. In Yoshua Bengio and Yann LeCun, editors, *1st International Conference on Learning Representations, ICLR 2013*, 2013.
- Alex Nichol, Joshua Achiam, and John Schulman. On first-order meta-learning algorithms. *arXiv preprint arXiv:1803.02999*, 2018.
- Aaron van den Oord, Yazhe Li, and Oriol Vinyals. Representation learning with contrastive predictive coding. *arXiv preprint arXiv:1807.03748*, 2018.
- Boris Oreshkin, Pau Rodríguez López, and Alexandre Lacoste. Tadam: Task dependent adaptive metric for improved few-shot learning. In *Advances in Neural Information Processing Systems*, pages 721–731, 2018.
- Eunbyung Park and Junier B Oliva. Meta-curvature. *Advances in Neural Information Processing Systems*, 32:3314–3324, 2019.
- Ben Poole, Sherjil Ozair, Aaron Van Den Oord, Alex Alemi, and George Tucker. On variational bounds of mutual information. In *International Conference on Machine Learning*, pages 5171–5180. PMLR, 2019.
- Hang Qi, Matthew Brown, and David G Lowe. Low-shot learning with imprinted weights. In *Proceedings of the IEEE conference on computer vision and pattern recognition*, pages 5822–5830, 2018.
- Sachin Ravi and Hugo Larochelle. Optimization as a model for few-shot learning. In *5th International Conference on Learning Representations, ICLR 2017, Toulon, France, April 24-26, 2017, Conference Track Proceedings*. OpenReview.net, 2017. URL <https://openreview.net/forum?id=rJY0-Kc11>.
- Avinash Ravichandran, Rahul Bhotika, and Stefano Soatto. Few-shot learning with embedded class models and shot-free meta training. In *Proceedings of the IEEE International Conference on Computer Vision*, pages 331–339, 2019.
- Andrei A Rusu, Dushyant Rao, Jakub Sygnowski, Oriol Vinyals, Razvan Pascanu, Simon Osindero, and Raia Hadsell. Meta-learning with latent embedding optimization. In *International Conference on Learning Representations*, 2019.
- Zhiqiang Shen, Zechun Liu, Zhuang Liu, Marios Savvides, Trevor Darrell, and Eric Xing. Un-mix: Rethinking image mixtures for unsupervised visual representation learning. In *AAAI*, 2022.
- Jianbo Shi and Jitendra Malik. Normalized cuts and image segmentation. *IEEE Transactions on pattern analysis and machine intelligence*, 22(8):888–905, 2000.
- Jake Snell, Kevin Swersky, and Richard Zemel. Prototypical networks for few-shot learning. In *Advances in Neural Information Processing Systems*, pages 4077–4087, 2017.
- Qianru Sun, Yaoyao Liu, Tat-Seng Chua, and Bernt Schiele. Meta-transfer learning for few-shot learning. In *Proceedings of the IEEE conference on computer vision and pattern recognition*, pages 403–412, 2019.

- Flood Sung, Yongxin Yang, Li Zhang, Tao Xiang, Philip HS Torr, and Timothy M Hospedales. Learning to compare: Relation network for few-shot learning. In *Proceedings of the IEEE Conference on Computer Vision and Pattern Recognition*, pages 1199–1208, 2018.
- Yonglong Tian, Dilip Krishnan, and Phillip Isola. Contrastive multiview coding. In *ECCV 2020*, pages 776–794. Springer International Publishing, 2020a.
- Yonglong Tian, Yue Wang, Dilip Krishnan, Joshua B Tenenbaum, and Phillip Isola. Rethinking few-shot image classification: a good embedding is all you need? In *European conference on computer vision*. Springer, 2020b.
- Yuandong Tian, Xinlei Chen, and Surya Ganguli. Understanding self-supervised learning dynamics without contrastive pairs. In Marina Meila and Tong Zhang, editors, *Proceedings of the 38th International Conference on Machine Learning, ICML 2021, 18-24 July 2021, Virtual Event*, volume 139 of *Proceedings of Machine Learning Research*, pages 10268–10278. PMLR, 2021.
- Michael Tschannen, Josip Djolonga, Paul K Rubenstein, Sylvain Gelly, and Mario Lucic. On mutual information maximization for representation learning. In *International Conference on Learning Representations*, 2020.
- Vikas Verma, Alex Lamb, Christopher Beckham, Amir Najafi, Ioannis Mitliagkas, David Lopez-Paz, and Yoshua Bengio. Manifold mixup: Better representations by interpolating hidden states. In *International Conference on Machine Learning*, pages 6438–6447. PMLR, 2019.
- Oriol Vinyals, Charles Blundell, Timothy Lillicrap, Daan Wierstra, et al. Matching networks for one shot learning. In *Advances in neural information processing systems*, pages 3630–3638, 2016.
- Feng Wang and Huaping Liu. Understanding the behaviour of contrastive loss. In *Proceedings of the IEEE/CVF Conference on Computer Vision and Pattern Recognition*, pages 2495–2504, 2021.
- Tongzhou Wang and Phillip Isola. Understanding contrastive representation learning through alignment and uniformity on the hypersphere. In *International Conference on Machine Learning*, pages 9929–9939. PMLR, 2020.
- P. Welinder, S. Branson, T. Mita, C. Wah, F. Schroff, S. Belongie, and P. Perona. Caltech-UCSD Birds 200. Technical Report CNS-TR-2010-001, California Institute of Technology, 2010.
- Zhirong Wu, Yuanjun Xiong, Stella X Yu, and Dahua Lin. Unsupervised feature learning via non-parametric instance discrimination. In *Proceedings of the IEEE conference on computer vision and pattern recognition*, pages 3733–3742, 2018.
- Shuo Yang, Lu Liu, and Min Xu. Free lunch for few-shot learning: Distribution calibration. In *International Conference on Learning Representations*, 2021.
- Chun-Hsiao Yeh, Cheng-Yao Hong, Yen-Chi Hsu, Tyng-Luh Liu, Yubei Chen, and Yann LeCun. Decoupled contrastive learning. *arXiv preprint arXiv:2110.06848*, 2021.
- Sung Whan Yoon, Jun Seo, and Jaekyun Moon. Tapnet: Neural network augmented with task-adaptive projection for few-shot learning. In *ICML 2019 (International Conference on Machine Learning)*. ICML, 2019.
- Sung Whan Yoon, Do-Yeon Kim, Jun Seo, and Jaekyun Moon. Xtarnet: Learning to extract task-adaptive representation for incremental few-shot learning. In *Proceedings of the 37th International Conference on Machine Learning, ICML 2020, 13-18 July 2020, Virtual Event*, volume 119 of *Proceedings of Machine Learning Research*, pages 10852–10860. PMLR, 2020.

- Zhongqi Yue, Hanwang Zhang, Qianru Sun, and Xian-Sheng Hua. Interventional few-shot learning. *Advances in Neural Information Processing Systems*, 33, 2020.
- Sangdoon Yun, Dongyoon Han, Seong Joon Oh, Sanghyuk Chun, Junsuk Choe, and Youngjoon Yoo. Cutmix: Regularization strategy to train strong classifiers with localizable features. In *Proceedings of the IEEE/CVF International Conference on Computer Vision*, pages 6023–6032, 2019.
- Jure Zbontar, Li Jing, Ishan Misra, Yann LeCun, and Stéphane Deny. Barlow twins: Self-supervised learning via redundancy reduction. In *Proceedings of the 38th International Conference on Machine Learning, ICML 2021, 18-24 July 2021, Virtual Event*, volume 139 of *Proceedings of Machine Learning Research*, pages 12310–12320. PMLR, 2021.
- Hongyi Zhang, Moustapha Cisse, Yann N Dauphin, and David Lopez-Paz. mixup: Beyond empirical risk minimization. In *International Conference on Learning Representations*, 2018.